THE JOURNAL OF PHYSICAL CHEMISTRY C

Article

An Environmental Friendly Nb-P-Si Solid Catalyst for Acid Demanding Reactions

Antonio Aronne, Martino Di Serio, Rosa Vitiello, Nigel J Clayden, Luciana Minieri, Claudio Imparato, Alessandro Piccolo, Pasquale Pernice, Paolo Carniti, and Antonella Gervasini

J. Phys. Chem. C, **Just Accepted Manuscript** • DOI: 10.1021/acs.jpcc.7b05886 • Publication Date (Web): 26 Jul 2017

An Environmental Friendly Nb-P-Si Solid Catalyst for Acid Demanding Reactions

Antonio Aronne[†*], Martino Di Serio[‡], Rosa Vitiello[‡], Nigel J. Clayden[fi], Luciana Minieri[†], Claudio Imparato[†], Alessandro Piccolo[∫], Pasquale Pernice[†], Paolo Carniti[§], and Antonella Gervasini[§*]

[†] Dipartimento di Ingegneria Chimica, dei Materiali e della Produzione industriale, Università di Napoli Federico II, Piazzale Tecchio, 80, I-80125, Napoli (Italy).

[‡] Dipartimento di Chimica, Università di Napoli Federico II, Complesso Universitario M.te S. Angelo, Via Cintia, 4, I-80126, Napoli (Italy).

[fi] School of Chemistry, University of East Anglia, Norwich, NR4 7TJ (UK)

[∫] Dipartimento di Agraria, Università di Napoli Federico II and Centro Interdipartimentale di Ricerca sulla Risonanza Magnetica Nucleare per l'Ambiente, l'Agro-Alimentare ed i Nuovi Materiali (CERMANU), Università di Napoli Federico II, Via Università 100, I-80055, Portici (Italy).

[§] Dipartimento di Chimica, Università degli Studi di Milano, Via Camillo Golgi, 19, I-20133, Milano (Italy).

ABSTRACT: Here we report the structural characteristics, the surface properties and the catalytic performances of a Nb-P-Si ternary oxide material ($2.5Nb_2O_5{\cdot}2.5P_2O_5{\cdot}95SiO_2$, 2.5NbP) in two reactions of importance for biomass valorisation and green industrial production: hydrolysis of inulin and esterification of oleic acid with polyalcohol for biolubricant production. High dispersion of the Nb centers, ascertained by UV-vis-DRS, ^{29}Si, ^{31}P and ^{1}H solid state NMR spectroscopy, is the key-point for the successful activity of 2.5NbP. *Intrinsic* and *effective* acidities of the sample were studied by FT-IR of adsorbed pyridine in absence and presence of water and by volumetric titrations of the acid sites in cyclohexane an in water, to enlighten the nature and amount of acid sites in different environment. For both studied reactions, 2.5NbP catalyst exhibits *water tolerant* acidic sites, mainly Brønsted ones, giving higher activity and better stability in the reaction medium than well-known niobium oxophosphate catalyst, which is considered one of the best *water-tolerant* acid catalysts.

INTRODUCTION

Catalysis is a central science in the development of new, safer and greener chemical processes. Solid acid catalysts are among the most widely used catalysts in industrial chemical processes. Beside to the development of more efficient, safer, and more environmentally friendly acid-catalysts, a typical desired property of the new acid catalysts is tolerance to water. In particular, biorefinery reactions take place in environments where high amounts of water vapour are present, or directly in liquid water (sugar polymer and carbohydrates transformations). Niobium oxophosphate ($NbOPO_4$, NbP) is an interesting solid acid catalyst (Ho <−8.2) with a high ratio of Brønsted (BAS) to Lewis (LAS) acidic sites,[1-4] which has been used as water-tolerant solid acid catalyst for various reactions of interest in biorefining, such as esterification,[5] hydrolysis,[6] dehydration,[4, 7-12] and alkylation.[13] The advantages of NbP stem from the recognized stability of Nb-O-P bonds towards hydrolysis and the presence of both kinds of acid sites at the surface. Besides the commercial source from the Companhia Brasileira de Metalurgia e Mineração (CBMM), NbP solid is usually obtained either by impregnation of hydrated niobium oxide with diluted orthophosphoric acid,[14] or by precipitation starting from niobium chloride using concentrated hydrochloric and orthophosphoric acid,[15] or by hydrothermal approaches using neutral[16] or cationic [9, 16, 17] surfactants. Hydrothermal methods allow the synthesis of mesoporous solids characterized by a high surface area though at the cost of being energy and or time consuming to prepare, requiring procedures with multiple steps. All the synthetic methods listed above need a strictly controlled pH. The prospect of both extending the use of this catalyst with other acid catalyzed reactions and improving its performance has stimulated the preparation of new catalytic systems based on niobium, phosphorus, and silicon,[18-19] as well as of multifunctional catalysts containing noble metals dispersed on NbP.[20-22] Performance improvements are aimed at modulating the distribution of acid sites and density at the surface by the addition of a third component (Si). So far the preparation of new catalytic systems based on niobium and

phosphorus has required the use of complex combined methods. Ziolek et al.[18] have introduced niobium and phosphorus into silicon mesoporous cellular foams, that were prepared by hydrothermal routes, either by sol-gel or by post-synthesis impregnation realizing the following molar ratios: Si/Nb = 64, Si/P = 50; Si/Nb = 64, Si/P = 10. Choi et al.[19] have prepared mesoporous niobium-phosphate-silicates characterized by Nb/P atomic ratios equal to 0.5 and 1 by a solvothermal method combined with solvent evaporation. These processes are complicated, they need several steps at temperatures higher than room temperature and they make use either of different precursors for P (orthophosphoric acid, triethylphosphate and diethylphosphatoethyltriethoxysilane) and for Si (tretraethylorthosilicate and diethylphosphatoethyltriethoxysilane)[19] or of toxic reactants such as 1,3,5-trimethylbenzene and toluene.[18] Recently, some of us have prepared amorphous niobium–phosphorus–silicon mixed oxide materials, with a molar ratio P/Nb = 1 and an Si content ranging from 95 to 80 mol%, by an innovative hydrolytic sol-gel route from phosphoryl chloride, niobium chloride and tetraethoxysilane, distinguished by the easy manipulation of precursors and wholly performed at room temperature.[23] These solids were characterized by both a very high degree of silicon crosslinking allowing phosphorus to be anchored through Nb-O-P bonds within the framework, and a high content of OH groups even at temperatures higher than 500 °C, that are mainly linked to phosphorus, making them strong acid solids.

In this work, the catalytic performances of the solid with the highest silicon content and higher dispersion of Nb, whose nominal composition can be expressed as $2.5Nb_2O_5 \cdot 2.5P_2O_5 \cdot 95SiO_2$ (2.5NbP), were exploited in two reactions of importance for biomass valorisation and green industrial production: hydrolysis of inulin and esterification of oleic acid with polyalcohols. It was shown that the catalyst exhibits intrinsic and effective acidities, measured both by FT-IR spectroscopy of pyridine adsorption in absence and presence of water and by acid-base titrations carried out in an apolar-aprotic solvent and in water.[24-26] The 2.5NbP structure was preserved after treatment in water giving only a partial removal of

strong Brønsted acid sites and some P-leaching. 2.5NbP presents better catalytic performances than the well-known acid catalyst NbP in both studied reactions proving its possible use as efficient water tolerant catalyst.

EXPERIMENTAL SECTION

Catalyst Preparation. The niobium-phosphorus-silicon mixed oxide **2.5NbP** material was prepared according to a sol-gel procedure previously described,[23] starting from phosphoryl chloride, $POCl_3$ (99%, Aldrich Chemical), niobium chloride, $NbCl_5$ (99%, Gelest), and tetraethoxysilane, $Si(OC_2H_5)_4$ (99%, Gelest), as starting materials. Amorphous gel-derived catalyst was obtained by annealing the dried gel at 500 °C (**2.5NbP-500**). The sample was prepared by slow heating at 5 °C·min^{-1} to the required temperature and held at this temperature for 1 h followed by quenching. To investigate the effective water tolerance of this sample, it was treated in water under vigorous stirring for 16 h at room temperature (**2.5NbP-500w**). Further details are available in the Supporting Information.

Catalyst Characterization. The amorphous nature of the 2.5NbP-500 was investigated by X-ray diffraction with a Philips X'PERT-PRO diffractometer by using monochromatized CuKα radiation (40 mA, 40 kV) with a step width of 0.013° 2θ. Ultra-violet and visible light diffuse reflection (UV-vis-DRS) spectra were recorded in the range of 190-800 nm on a double beam Jasco spectrophotometer. Barium sulfate was used a reflectance standard. The measured intensity was expressed as the value of the Kubelka-Munk function F(R).

^{29}Si-, ^{31}P- and ^{1}H-NMR spectra were acquired by Direct Polarization (DP) Magic Angle Spinning (MAS) technique with a Bruker AVANCE 300 (Bruker Biospin, Milan, Italy) magnet equipped with a 4-mm wide-bore MAS probe and operating at ^{29}Si, ^{31}P and ^{1}H resonating frequencies of 59.6, 121.5 and 300.3 MHz, respectively.

Samples were packed in 4 mm zirconia rotors with Kel-F caps and spun at 10000±1 Hz. ^{29}Si spectra were acquired using 5352 data points, 1000 scans, a recycle delay of 180 s and a spectral width of 400 ppm (23809 Hz); ^{31}P spectra were acquired with 2914 data points, 500 scans, a recycle delay of 150 s and a spectral width of 400 ppm (48543 Hz); ^{1}H spectra were collected with 5352 data points, 16 scans, a recycle delay of 60 s and a spectral width of 333 ppm (99954 Hz). High power proton decoupling was applied with the ^{31}P acquisition only using a 30 ms long TPPM15 composite pulse (-0.5 dB power attenuation), that led to signals enhancement owing to the minimization of long-range proton coupling.

Each spectrum was processed using Bruker Topspin software (v.2.1). In particular, the free induction decays (FID) of ^{29}Si and ^{31}P spectra were Fourier Transformed (FT) by applying a 8 and 4 k zero filling and adopting an exponential filter function, with a line broadening of 100 and 50 Hz, respectively. No zero filling and apodization were applied during the FT of ^{1}H spectrum. Each spectrum was phase and baseline corrected.

Morphologic characteristics of 2.5NbP-500 were studied by N_2 adsorption and desorption isotherms measured at liquid nitrogen temperature with an automatic surface area analyzer (Sorptomatic 1900 instrument). Prior to the measurements, thermal activation at 150 °C for 16 h (overnight) was performed under vacuum.

Lewis and Brønsted acid sites (LAS and BAS) of 2.5NbP-500 as well as their tolerance to water, were investigated by Fourier Transform Infrared Spectroscopy (FT-IR) (Biorad FTS-60A) using pyridine as probe molecule both in vapor phase and aqueous solution. The samples were pressed into 10-15 mg self-supporting disk (0.65 cm^2 geometrical area) and before each analysis they were activated at 150 °C for 2 h under air. After outgassing for 30 minutes in high vacuum, the sample was contacted with pyridine vapors at room temperature for 10 minutes or, alternatively, a 1x10^{-3} M pyridine aqueous solu-

tion was dropped on self-supporting disks under argon flow. After pyridine adsorption, the sample was outgassed for 30 minutes in high vacuum at several temperatures (i.e. RT, 50, 100 °C) without the possibility to realize higher temperatures due to the violent evaporation of water that caused the rupture disk. BAS and LAS concentration (expressed as meq g_{cat}^{-1}) was determined by integrating the peaks at 1540 and 1448 cm^{-1}, respectively, of the spectra collected after outgassing at 100 °C.

The amount of acid sites of 2.5NbP-500 was measured by using 2-phenylethylamine (PEA) as basic probe in cyclohexane for the *intrinsic* acidity (I.A.) and in water for the *effective* acidity (E.A.) at 30 °C by working in an adsorption HPLC line specifically assembled for this purpose.[4, 25, 26] Further details are available in the Supporting Information.

Activity Tests. The tests of the catalytic hydrolysis of inulin were performed in water in a glass slurry batch reactor (Syrris, Atlas, UK) with magnetic stirrer at constant rate of 800 rpm under increasing temperature from 50 to 90 °C (0.12 °C·min^{-1}, for a total of 6 h of reaction).

Inulin, in powder form, was a commercial pure product (Carlo Erba, RPE) with a number-averaged degree of polymerization (DPn) of 25, evaluated on the basis of the ratio of fructose to glucose residues in inulin and considering that each molecule of inulin contains one glucose residual (at the chain end point). The catalyst sample (ca. 0.3 g sieved between 20-80 mesh) was treated at 120 °C overnight (ca. 16 h) in oven under air atmosphere. Inulin (1.5 g) was dissolved in 150 mL water (concentration, 55 mM). For each catalyst, two different catalytic tests were performed by using i) fresh and dried catalyst samples and ii) catalyst sample stabilized in water overnight (at r.t.) to verify the activity of the sample after water stabilization. In detail, the weighted and dried sample was put in the reactor filled with water where it was maintained for 16 h (overnight) at room temperature under gentle stirring, then, a weighted amount of inulin was added to obtain an inulin solution at the desired concentration; then, the reaction started, while the temperature was allowed to increase (0.12 °C/min).

The yield to reducing sugars (corresponding to the extent of reaction and called *inulin conversion* herein after below) was evaluated as the ratio between the reducing sugars produced and the reducing sugars at complete hydrolysis of substrate. The selectivity to fructose and glucose was determined on the basis of the ratio between fructose or glucose formed and the reducing sugars produced.

The reaction was followed by measuring the total reducing sugars by the classical colorimetric Nelson-Somogyi method by using copper(II) sulfate pentahydrate ($Cu(SO_4)\cdot 5H_2O$, Carlo Erba, RPE) and ammonium molybdate ($(NH_4)6MoO_{14}\cdot 4H_2O$, Carlo Erba, RPE) salts. The blue complex formed was analyzed and quantified at 520 nm. Moreover, the presence of glucose and fructose was determined by a Boehringer enzymatic assay technique.

The kinetic coefficients at the average temperature Tm between two samplings (k_{Tm}) were calculated by the Eq. (1):

$$k_{Tm} = (\Delta C/\Delta t) / C_m \qquad \text{Eq. (1)}$$

where Δt is the time variation between two samplings (Δt = 30 min and ΔT = 5 °C); ΔC is the variation of bond concentration between two samplings; C_m is the average bond concentration between two samplings.

The esterification reaction was carried out in a 100 mL glass reactor equipped with a magnetic stirrer. Oleic acid and the catalyst (previously dried at 110 °C for 3h) were initially loaded into the reactor. The reactor was heated to the desired temperature and then polyalcohol loaded into the reactor with a constant flow of nitrogen (20 NL/h) for a continuous stripping of the water from the reactive mixture. During each experimental run, samples were periodically withdrawn, in order to determine the evolution of the reaction products composition during the time. The withdrawn samples of the reaction mixture were analyzed by a standard acid–base titration procedure for the evaluation of the free residual acidity. The operative conditions for all the esterification runs were: temperature 180 °C, alcohol: acid molar ra-

tio 1: 2, catalyst concentration 1% wt (based on reaction mixture). The catalysts after the reaction were recovered by centrifugation and in some cases were reused to study the stability to deactivation.

RESULTS AND DISCUSSION

Structural Characteristics. An amorphous gel-derived catalyst (2.5NbP-500) obtained by annealing the 2.5NbP dried gel at 500 °C for 1 h and the same catalyst treated at room temperature for 16 h in water (2.5NbP-500w) were studied in order to verify its effective water tolerance.

The analysis of the powder X-ray diffraction (PXRD) pattern of 2.5NbP-500 clearly shows its amorphous nature as well as the lack of any segregated crystalline phase (Figure 1).

UV-vis-DRS spectroscopy was used to determine the coordination geometry and chemical arrangement of the niobium species on the surface of the investigated samples since the band gap energies which can be derived from the spectra are known to depend on the coordination symmetry of the niobium involved with the electronic transition. Figure 2 shows the UV-vis-DRS spectra of 2.5NbP-500 and 2.5NbP-500w along with the spectra of NbP and Nb_2O_5 reference samples, as well as the corresponding Tauc equation plots.[27] Band gap energies (E_g) were found using these plots from the intercept of the extrapolated linear absorption edge with the energy axis. The value found for Nb_2O_5 (E_g = 3.14 eV, 395 nm) is very close to the literature value reported for crystalline Nb_2O_5 having a structure formed by corner-sharing NbO_6 octahedra in which a large fraction of niobium atoms lies in sites characterized by high coordination symmetry.[28] Therefore the above optical band gap is related to charge transfer (CT) arising from excitation of an electron of the 2p oxygen valence band to the empty 4d niobium conduction band belonging to high symmetry NbO_6 octahedra.[29, 30] CT involving niobium atoms belonging to Nb polyhedra characterized by a lower symmetry, low distorted NbO_6 octahedra (i.e. edge-sharing NbO_6 octahedra), high distorted NbO_6 octahedra (i.e. face-sharing NbO_6 octahedra, disordered NbO_6 octahe-

dra), high symmetry NbO_4 tetrahedra (i.e. corner-sharing NbO_4 tetrahedra), distorted NbO_4 tetrahedra (i.e. edge- or face-sharing NbO_4 tetrahedra, disordered NbO_4 tetrahedra), isolated NbO_4 tetrahedra, are associated with progressively higher E_g values.[29,30] Two optical band gaps were discovered for NbP ($E_{g,1}$ = 3.71 eV, $E_{g,2}$ = 4.80 eV) indicating the presence in this sample both of low symmetry NbO_6 octahedra and disordered NbO_4 tetrahedra as a consequence of its amorphous nature. The same E_g was observed for 2.5NbP-500 and 2.5NbP-500w (E_g = 3.86 eV) demonstrating that the water treatment does not modify the distribution of surface Nb species.

The UV-vis spectrum of Nb_2O_5 shows the typical feature of a polycrystalline sample of niobium oxide with absorptions at about 257, 310, and 350 nm that are related to NbO_6 octahedra with different symmetry: face-sharing, edge sharing and corner-sharing, respectively. The NbP spectrum reflects its amorphous nature with features at about 270 and 208 nm that are related to CT relating to NbO_6 octahedra and NbO_4 tetrahedra, respectively. The residual absorption in the 300-350 nm range indicates the presence also of high symmetry NbO_6 octahedra.

Curves fitting of 2.5NbP-500 and 2.5NbP-500w spectra were performed (Figure S1 of Supporting Information) for a better insight in their similarities confirming that the water treatment does not change the distribution of surface NbO_x species and the results are summarized in Table 1. For each sample CT transitions associated with isolated NbO_4 tetrahedra (~ 200 nm), low distorted NbO_4 tetrahedra (~ 230 nm), high distorted NbO_6 octahedra (~ 265 nm) and low distorted NbO_6 octahedra (~300 nm) are seen.[28-30] This assignment also agrees with the recent interpretation proposed by Tranca et al.[31] for silica-supported niobium oxide catalysts. They, based on DFT calculations, assigned the UV band at about 260 nm to penta-coordinate niobium atoms, that indeed can be seen as high distorted NbO_6 octahedra.

A high degree of silicon cross-linking occurs in the siloxane network for both the 2.5NbP-500 materials as a consequence of the sol-gel procedure used, as revealed by the ^{29}Si NMR (Figure 3). Cluster-

ing of NbO_6 octahedra containing Nb-O-X (X = Si and/or P) bridges and of NbO_4 tetrahedra consequently can occur. Notably, the formation of these bridges requires the occurrence of different kinds of distorted NbO_6 octahedra, while the stabilization of the four-fold coordination of Nb^{5+} plays a key role in realizing the interconnected network in which the cross-condensation between Nb- and P-units allows the formation of P-O-X (X = Nb and/or P) bridges, in agreement with the UV-vis analysis.

^{29}Si, ^{31}P, and ^{1}H solid state NMR spectra of 2.5NbP-500 and 2.5NbP-500w are shown in Figures 3 a), 3b), and 3c) respectively. Prior to ^{1}H MAS NMR experiments, the samples were dehydrated at 100 °C for one day and then introduced into the sample holder using a glove-box. Distinct chemical shifts ranges are seen in both the ^{29}Si and ^{31}P NMR spectra for the various degrees of connectivity of the structural units as described by the Q_N notation[32, 33] where N is the number of bridging oxygen of the tetrahedral unit.

Overall the ^{29}Si NMR data indicate extensive cross-linking with 70.0% Q_4 units and 25.0% Q_3 units for 2.5NbP-500 and 69.2% Q_4 units and 26.6% Q_3 units for 2.5NbP-500w. Consequently the observation of only minor differences between the ^{29}Si NMR spectra of the materials before and after exposure to water indicates, as expected, the silicate network is essentially unaffected by the water exposure. In contrast significant differences were observed in the ^{31}P NMR spectra before and after exposure to water as can be seen from the detailed curve fitted resonances, (Table 2) implying a modification in the network connectivity. Notably there is a marked decrease in the relative intensity of the Q_1' resonance at ~ -9 ppm which has been assigned to a terminal type phosphate.

First and foremost though it is important to recognize there remains significant intensity associated with chain type phosphates with the Q_2' and Q_3' resonances. This is of particular importance as it establishes the majority of the phosphorus is still anchored into the silicate matrix. Unlike all previous samples of silico-phosphates which have shown the creation of monomeric phosphate, and hence detach-

ment from the silicate network upon long exposure to even atmospheric moisture. The decrease in the amount of Q_1' can be understood either in terms of further cross-linking despite the hydrolytic conditions or the loss of terminal phosphate groups through leaching. Of these explanations the latter is the more plausible and assuming this is the only source of loss of phosphorus it can be estimated that 32 % of the total phosphorus has been lost.

Owing to the chemical nature of the materials in question, ^{1}H NMR will highlight two types of environment in the sample, hydroxyl groups and bound water. The hydroxyl groups may be terminal or bridging and associated with silicon, phosphorus or niobium (X-OH, X = Si, P and Nb; X-O(H)-Y, with X, Y = Si, P and Nb). Assignment of the resonances to a particular environment is fraught with difficulty though generally terminal Si-OH are found around 2 ppm except inaccessible isolated ones may be found as shielded as 1.1 ppm[34] while resonances around 5 ppm could be any bridging Si-O(H)-X (X = P, Nb). Terminal X-OH (X = P, Nb) are expected to be more shielded and may be found in the range 0-1 ppm.[35] A further complication is that hydrogen bonding of terminal type hydroxyl will lead to deshielding with the result ab initio calculations predict even Si-OH can be as deshielded as 5-11 ppm.[36] In view of the uncertainty in the assignments any explanation for the changes in the ^{1}H NMR spectrum on exposing the 2.5NbP material to water must be tentative. Nevertheless, the changes can be understood in terms of the known hydrolytic instability of surface cross-linking bonds such as Si-O-P.

Previous ^{29}Si and ^{31}P MAS NMR has established a structure for the 2.5 NbP-500 material based on a silicate network with cross-linking between the phosphorus and niobium anchoring the phosphorus through the niobium to this network P-O-Nb-O-Si. Some evidence was also found in the earlier work for Si-O-P since small changes were seen in the ^{31}P NMR spectrum on exposure to atmospheric moisture. It should be noted that the very fact these changes were small provided strong evidence for the indirect anchoring of the phosphorus through the niobium. The silicate network is characterised, through terminal

Si-OH, by the resonances seen at 2 ppm. Less clarity is afforded by the single broad resonance at 5.5 ppm. In all likelihood this represents a heterogeneous mix of environments involving the phosphorus and niobium such as P-O(H)-Nb. These hydrogens would represent the source of the Brønsted acidity in non-aqueous solvents. Indeed in the case of alumina impregnated with niobium oxide, it has been proposed that a broad resonance at 8 ppm but 10 ppm wide corresponds to Nb-O(H)-Nb Brønsted acid sites. Such a broad line would encompass the ^{1}H chemical shifts seen for 2.5 NbP-500.[37] Upon exposure to water the resonance at 2 ppm remains unchanged, as expected given the inertness of silicate networks to hydrolysis. However, new resonances appear around 1.8 ppm typical of terminal Si-OH. The most plausible explanation of these is the hydrolysis of any Si-O-P formed during the synthesis. Changes in the resonance at 5.5 ppm assigned to the hydrogen associated with the phosphorus and niobium must be related to hydrolytic instability of the cross-linking, however, it is clear from the ^{29}Si that bulk material is largely unaltered. Again, it is probable that the broad resonance centered at 4 ppm will represent a variety of P-OH and Nb-OH environments while the observed increase in ^{1}H shielding is consistent with hydrolysis of X-O-Y (X, Y = P, Nb) giving rise to X-OH and Y-OH. Further support for this hydrolysis is provided by the greater intensity seen for the 4 ppm resonance in the sample after exposure to water compared with the 5.5 ppm resonance before water exposure.

Morphologic Characteristics. The isotherms of N_2 adsorption and desorption at 77 K collected on 2.5NbP-500 indicate its porous character and high surface area (Figure 4).

The adsorption isotherm is a combination of type I (solid with micropores) and IV (solid with mesopores), according to the IUPAC classification. The observed hysteresis loop at around P/P°=0.5 is characteristic for type H4 loop. Type H4 hysteresis is associated with particles containing small pores including the micropores. In addition, the first part of the adsorption isotherm is typical of samples containing micropores (< 2 nm), that is, high N_2 adsorption at very low P/P° values and sharp knee of the

isotherm (B point, which indicates the completion of the monomolecular N_2 layer). Thus it is apparent that 2.5NbP-500 doesn't have a single pore type but instead a combination of micropores and mesopores. The surface area of 2.5NbP-500 was calculated by the classical 2-BET and 3-BET equations obtaining surface area values of 524 and 532 $m^2 \cdot g^{-1}$, respectively. Positive value for the C_{BET} constants and an average number of N_2 layers on the whole surface of 2.6 were obtained. The results suggest a predominantly mesoporous character for 2.5NbP-500, though with some micropores. The total porosity evaluated by the Gurvich rule was 0.33 $cm^3 g^{-1}$, that comprises interparticle and intraparticle porosity, of this the mesopore volume determined by BJH model equation was 0.14 $cm^3 \cdot g^{-1}$. The mesopore size is centered at 3.20 nm (Figure 4 a') and the micropore volume is 0.12 $cm^3 \cdot g^{-1}$, as determined by the Dubinin Raduskevich equation (Figure 4 a''). For sake of comparison, the N_2 isotherms of adsorption-desorption of NbP together with its morphological properties are reported in Figure S2 of Supporting Information.

Acidity Determinations. The acid properties of 2.5NbP-500 and of NbP, used as reference sample, were determined by two approaches: spectroscopic determination of the nature (BAS or LAS) of acid sites by FT-IR of adsorbed pyridine and liquid-solid acid-base titrations using 2-phenyl-ethyl-amine (PEA) as basic probe molecule. Figure 5 shows the FT-IR spectra of pyridine adsorption on 2.5NbP-500 recorded after pyridine desorption at 100°C in the interval 1700 to 1350 cm^{-1}. The two spectra refer to pyridine adsorption in gas-phase and in aqueous solution (10^{-3} M). Both BAS and LAS could be observed under the two different conditions, absence and presence of water. Table 3 reports the quantitative results of the spectroscopic adsorption of pyridine on 2.5NbP-500 and comparatively on NbP. In absence of water, a similar amount of LAS were found for 2.5NbP-500 and NbP, despite that the nominal content of Nb is much lower on 2.5NbP-500 than on NbP (about 7 and 47 Nb wt%, respectively). This result can be related to a better dispersion and accessibility of Nb sites occurring in the studied catalyst

than in NbP, as proved by the UV-vis characterization showing the presence of NbO_4 tetrahedra with a low distortion degree (isolated) dispersed into the mixed Si-P framework of 2.5NbP-500. According to ^{1}H MAS NMR analysis, the higher presence of BAS on 2.5NbP-500 than on NbP (LAS/BAS, 1.06 and 2.10 for 2.5NbP-500 and NbP, respectively) was expected as two types of environment were found for 2.5NbP-500: hydroxyl groups and bound water. The former is related to terminal X-OH, with X = Si, P and Nb, the latter relates to bridging hydrogen X-O(H)-Y, with X, Y = Si, P and Nb, formed by H-bonding between water and X-O-Y bridging oxygen. It is noteworthy that in this condition (absence of water) there is a high contribution of Si-OH groups.

More interestingly, in the presence of water for 2.5NbP-500 both LAS and BAS concentrations decrease but this trend is more pronounced for LAS giving a LAS/BAS ratio equal to 0.39. The strong decrease of LAS occurring in 2.5NbP-500 in comparison with NbP can be related to the greater hydrolysis rate of NbO_4 tetrahedra with respect to the NbO_6 octahedra, producing Nb-OH terminal groups. Support for this hydrolysis is also provided by the comparison of ^{1}H NMR of the sample before and after exposure to water. This phenomenon partially counteracts the missed contribution of the Si-OH groups and the loss of P-OH terminal groups due to P leaching, which does not occur in the same extent for NbP, giving a LAS/BAS four times greater than 2.5NbP-500. In other words, in the presence of water the BAS concentration in 2.5NbP-500 is about twice the value for NbP.

Concerning the liquid-solid acid-base titrations, PEA was chosen for its high basicity and easy detection in the UV-region (λ_{max} = 254 nm). The titrations were carried out in two liquids with different physical properties: cyclohexane with apolar and aprotic properties and water with polar, protic, and solvating properties. Owing to the different characteristics of the two liquids, titrations in cyclohexane allowed the determination of the so called *intrinsic* acidity of the samples. In contrast, titrations in water gave the *effective* acidity of the samples, as water is able to have specific chemical interactions with giv-

en functional groups of the surface and to cause hydrolytic action.[24-26] All the PEA adsorption isotherms collected at 30 °C in the two liquids are shown in Figure 6. All the isotherms obtained were Langmuir in type for both the solvents, the differences between the attained *plateau* of adsorption between the first and second runs were due to the presence of higher or lower numbers of strong acid sites on the two samples.

The acidity measured in cyclohexane was much higher on 2.5NbP-500 (0.600 mequiv·g^{-1} of acid sites) than on NbP (0.403 mequiv·g^{-1} of acid sites), with a high and similar percentage of strong acid sites in both samples (86%). Different results were obtained by titrating the sample acidity in water; the number of acid sites titrated was greatly decreased on 2.5NbP-500 (0.126 mequiv·g^{-1} of acid sites) and only slightly on NbP (0.350 mequiv·g^{-1} of acid sites), ca. 79 % and 13 % of acidity decrease, respectively, in comparison with the titrations performed in cyclohexane. The *effective* acidity was higher on NbP (31% of strong acid sites in water) than on 2.5NbP-500, which does not show any strong acidity in agreement with the above trends of LAS/BAS ratio. In the presence of water a substantial reduction of P-OH occurs for 2.5NbP-500 leaving on its surface weak BAS, mainly Si-OH and Nb-OH that are not able to adsorb PEA because they are engaged with water coordination (H-bonding). Then, the lower average acid strength of 2.5NbP-500 surface in comparison with the acid surface of NbP could give benefits for improving the catalyst stability in given catalytic reactions in which NbP has been already studied (fructose dehydration, cellobiose hydrolysis, etc.). The high acid strength of NbP surface provoked irreversible adsorption of reagents/intermediates with formation of humic material responsible of a fast catalyst deactivation.[4, 25]

Catalytic Activity Tests. Inulin is a natural polysaccharide consisting of linear chains of fructose residues linked by β-1,2 bonds and terminated with a sucrose residue; it acts as energy reserve in various plants (e.g., chicory and Jerusalem artichoke) that can grow in hardly exploitable marginal areas. The

exploitation of such cultivations and the resulting inulin extraction make possible production of syrups with higher fructose content than from other traditional processes, like glucose isomerization.[38-40] The reaction of inulin hydrolysis can be carried out by employing inorganic catalysts or biocatalysts (inulinases). Among inorganic catalysts, protonic acid solid catalysts (with BAS sites) are promising. NbP has long been used in several reactions aimed at improving the value of saccharides and polysaccharides, thanks to its BAS and LAS at the surface. When NbP is used without any severe thermal treatment, it is highly protonic acid and it can catalyze the same reactions of acid catalysts in homogeneous liquid phase. Inulin hydrolysis can be easily followed by measuring the total reducing sugar concentration, formed by the breaking of the bonds between the monosaccharide units that form this organic polymer. The time course of the inulin hydrolysis was studied in water as a function of time/temperature in the 50-90 °C interval by adding the dry catalyst samples in comparison with the samples stabilized in water for long time before the reaction. In so doing, the intention was to control the stability of the samples to the hydrolytic action of water, i.e., the stability of the Nb-O-P bonds.

Figure 7 shows the increasing trends in the formation of the total reducing sugars for both the NbP (Figures 7 a, b, and c) and 2.5NbP-500 (Figures 7 a', b', and c') samples in the studied temperature interval. Inulin hydrolysis started at ca. 67-70 °C (corresponding to 2.5-3 h of reaction) and reached more than 80% using either of the fresh catalysts at the highest reaction temperature (90 °C corresponding to 6 h of reaction). It is noteworthy to observe that the curves of 2.5NbP-500 (fresh and water stabilized catalysts, Figure 7 a') are perfectly superposed, indicating that the sample did not suffer any deactivation of the catalytic sites by water. The same observation does not hold for NbP (Figure 7 a), in this case the curve for the water stabilized NbP sample lies under that of the fresh NbP sample at each time/temperature of reaction. In all likelihood, some hydrolytic effect of water on NbP has occurred that has caused phosphorus leaching. Indeed, leaching experiments from aqueous solutions in the presence of

NbP and 2.5NbP-500 have indicated the loss of phosphorus of ca. 15% for NbP (P nominal content, 6.94 wt%) and of 28% for 2.5NbP-500 (P nominal content, 2.30 wt%), with higher values in hot water. This observation is in contrast with the known properties of NbP (stability and insolubility in water) and further studies will be necessary in view of the real application of these materials in aqueous catalysis. The total reducing sugars analyzed correspond to the monosaccharides, glucose and fructose, the increasing inulin conversion led to higher selectivity towards these monosaccharides. Indeed, the molar ratio of monosaccharides to total sugars produced at the highest inulin conversion attained was ≥0.9 for 2.5NbP-500 (Figure 7 b') and between 0.8-0.9 for NbP (Figure 7 b). These figures depict unique trends in the ratio of fructose plus glucose to reducing sugars for each catalyst regardless of the catalyst treatment (fresh or water stabilized).

Moreover, the ratio of fructose to glucose (F/G) produced by the hydrolysis was much higher at low inulin conversion and the ratio diminished with conversion, as expected. Activation parameters for the two catalysts were determined from Arrhenius plots (Figures 7 c and 7 c') for NbP and 2.5NbP-500, respectively) using the rate constants calculated at T_m (average temperature on 30 min of reaction) (Table 4). Two distinct parallel lines can be seen for the fresh and water stabilized NbP catalyst, while a single line can be fitted to the data for the fresh and water stabilized 2.5NbP-500 catalyst. The calculated apparent activation energy values did not differ significantly for the two catalyst samples (E_a around 143 $kJ \cdot mol^{-1}$ and ln A around 47).

Esterification of fatty acids with high boiling polyalcohols is a potentially valuable reaction for industry because the esters formed can be used as biolubricants.[41] Alternatively, esterification of fatty acids with methanol can be used to produce biodiesel. A great number of heterogeneous catalysts have been proposed for these reactions.[42-46] Recently, NbP has also been used as esterification catalyst for fatty acids with alcohols (methanol, ethanol, 1-butanol).[5] Here the esterification of oleic acid (OA) and

nonanoic acid (NA) with polyalcohols (1,3 propandiol (PD), trimethylolpropane (TMP), pentaerythritol (PE)) by NbP and 2.5NbP-500 catalysts was studied. Nonanoic acid is not a natural fatty acid but it is the coproduct of azelaic acid synthesis from oleic acid.[47]

The conversion of OA and NA is reported in Figure 8 for both catalysed and non-catalysed runs. One contribution to the difference in the reaction rate observed for the different substrates is the higher concentration of fatty acids in the reaction mixture for TMP and PE in respect to PD because a stoichiometric fatty acid/alcohol molar ratio was used. A higher concentration of fatty acids will favour an autocatalytic mechanism, mainly at the beginning of the reaction. Although the activity of NbP is greater than the activity of 2.5NbP-500 in every case, in agreement with the higher effective acidity of NbP, of more importance is the greater stability of the 2.5NbP-500 catalyst. From Figure 8 d it is evident that the recovered NbP has lower activity than the corresponding 2.5NbP-500 after the first use and the activity of 2.5NbP-500 catalyst remains constant at least after 3 reuses (see Figure 8 e). Also in the case of esterification the catalyst stability is favoured by the lower average acid strength of 2.5NbP-500 surface in comparison with that of NbP. The lower acid strength of 2.5NbP-500 than that of NbP depends from its structure, as it is not a mere dispersion of NbP in a silica matrix but it is a ternary system with Si-O-Nb-O-P bridges, in which the components are uniformly dispersed at the molecular level.

CONCLUSIONS

The studied Nb-P-Si ternary oxide material is characterised by a very high polymerization degree giving a silicate matrix in which phosphate units are stably anchored by niobium bridges. Niobium can then have high dispersion in the silicate matrix giving a high LAS concentration, despite the low niobium content in the composition. The peculiar acidic properties of this solid, the high concentration of both BAS and LAS sites, were for the most part preserved after treatment in water, especially concern-

ing BAS sites. Only a partial removal of strong BAS and some phosphorus leaching occur, leading to some loss of the less polymerised Q_1' units. Despite these surface modifications after water contact, the BAS concentration in the Nb-P-Si material remained about twice the value for NbP, showing the high water-tolerance of the acid sites of the ternary oxide. On the other hand, the titrated *effective* acidity of the Nb-P-Si material was lower than that of NbP because of the presence on its surface of weak BAS sites, mainly Si-OH and Nb-OH. Consequently, it showed excellent catalytic performances in two important reactions which are known requiring acid sites: the hydrolysis of inulin and the esterification of oleic acid with polyalcohols. Indeed, higher conversion and selectivity to monosaccharides (fructose and glucose) were observed for the Nb-P-Si catalyst stabilized for long time in water with respect to NbP. Moreover, the moderate acidity of the Nb-P-Si catalyst allows keeping alive its activity for more reuses in the esterification of oleic acid with polyalcohols.

Therefore, this new ternary oxidic sample can be considered as an interesting material in the emerging field of heterogeneous acid catalysis in water, or involving water or polar-protic species as solvent, reagent, or product, in view of the development of new catalysts for *green* reactions.

ASSOCIATED CONTENT

Supporting Information

The Supporting Information is available free of charge on the ACS Publications website. Details concerning the preparation procedure of the studied material, the characterization of its surface acidic properties, the curves fitting of 2.5NbP-500 and 2.5NbP-500w UV-vis DRS spectra, as well as the N_2 adsorption-desorption isotherms of NbP and its main morphological data (PDF).

AUTHOR INFORMATION

Corresponding Authors

*To whom correspondence should be addressed:

Antonio Aronne, Tel. +390817682556, E-mail: anaronne@unina.it;

Antonella Gervasini, Tel. +390250314254, E-mail: antonella.gervasini@unimi.it.

Notes

The authors declare no competing financial interest.

ACKNOWLEDGMENTS

The authors thank Dr. Pierluigi Mazzei and the Centro Interdipartimentale di Ricerca sulla Risonanza Magnetica Nucleare per l'Ambiente, l'Agro-Alimentare ed i Nuovi Materiali (Università di Napoli Federico II) for MAS NMR measurements. Dr. Filippo Bossola from Istituto di Scienze e Tecnologie Molecolari (ISTM-CNR) of Milano is gratefully acknowledged for the FT-IR experiments.

REFERENCES

(1) Martins, R. L.; Schitine, W. J.; Castro, F. R. Texture, surface acidic and catalytic properties of niobium phosphate. *Catal. Today* **1989**, *5*, 483-491.

(2) Okuhara, T. Water-tolerant solid acid catalysts. *Chem. Rev.* **2002**, *102*, 3641-3666.

(3) Ziolek, M. Niobium-containing catalysts - the state of the art. *Catal. Today* **2003**, *78*, 47-64.

(4) Carniti, P.; Gervasini, A.; Biella, S.; Auroux, A. Niobic acid and niobium phosphate as highly acidic viable catalysts in aqueous medium: Fructose dehydration reaction. *Catal. Today* **2006**, *118*, 373-378.

(5) Bassan, I. A. L.; Nascimento, D. R.; San Gil, R. A. S.; Pais da Silva, M. I.; Moreira, C. R.; Gonzalez, W. A.; Faro Jr., A. C.; Onfroy, T.; Lachter, E. R. Esterification of fatty acids with alcohols over niobium phosphate. *Fuel Process. Technol.* **2013**, *106*, 619-624.

(6) Marzo, M.; Gervasini, A.; Carniti, P. Hydrolysis of disaccharides over solid acid catalysts under green conditions. *Carbohydr. Res*. **2012**, *347*, 23-31.

(7) Rao, G. S.; Rajan, N. P.; Pavankumar, V.; Chary, K. V. R. Vapour phase dehydration of glycerol to acrolein over $NbOPO_4$ catalysts. *J. Chem. Technol. Biotechnol.* **2014**, *89*, 1890-1897.

(8) Ordomsky, V. V.; Sushkevich, V. L.; Schouten, J. C.; van der Schaaf, J.; Nijhuis, T.A. Glucose dehydration to 5-hydroxymethylfurfural over phosphate catalysts. *J. Catal.* **2013**, *300*, 37-46.

(9) Zhang, Y.; Wang, J.; Ren, J; Liu, X.; Li, X.; Xia, Y.; Lu, G.; Wang, Y. Mesoporous niobium phosphate: an excellent solid acid for the dehydration of fructose to 5-hydroxymethylfurfural in water. *Catal. Sci. Technol.* **2012**, *2*, 2485-2491.

(10) Armaroli, T.; Busca, G.; Carlini, C.; Giuttari, M.; Raspolli Galletti, A. M.; Sbrana, G. Acid sites characterization of niobium phosphate catalysts and their activity in fructose dehydration to 5-hydroxymethyl-2-furaldehyde. *J. Mol. Catal. A Chem.* **2000**, *151*, 233-243.

(11) West, R. M.; Braden, D. J.; Dumesic, J. A. Dehydration of butanol to butene over solid acid catalysts in high water environments. *J. Catal.* **2009**, *262*, 134-143.

(12) de La Cruz, M. H. C.; Rocha, Â. S.; Lachter, E. R.; Forrester, A. M. S.; Castro Reis, M.; San Gil, R. A. S.; Caldarelli, S.; Farias, A. D.; Gonzalez, W. A. Investigation of the catalytic activity of niobium phosphates for liquid phase alkylation of anisole with benzyl chloride. *Appl. Catal. A Gen.* **2010**, *386*, 60-64.

(13) de la Cruz, M. H. C.; da Silva, J. F.C.; Lachter, E. R. Catalytic activity of niobium phosphate in the Friedel–Crafts reaction of anisole with alcohols. *Catal. Today* **2006**, *118*, 379-384.

(14) Okazaki, S.; Kurosaki, A. Acidic properties and catalytic activities of niobic acid treated with phosphoric acid. *Catal. Today* **1990**, *8*, 113-122.

(15) Sørensen, D. R.; Nielsen, U. G.; Skou, E. M. Solid state ^{31}P MAS NMR spectroscopy and conductivity measurements on $NbOPO_4$ and H_3PO_4 composite materials. *J. Solid State Chem.* **2014**, *219*, 80-86.

(16) Mal, N. K.; Fujiwara, M. Synthesis of hexagonal and cubic super-microporous niobium phosphates with anion exchange capacity and catalytic properties. *Chem. Commun.* **2002**, 2702-2703.

(17) Sarkar, A.; Pramanik, P. Synthesis of mesoporous niobium oxophosphate using niobium tartrate precursor by soft templating method. *Micropor. Mesopor. Mat.* **2009**, *117*, 580-585.

(18) Stawicka, K.; Trejda, M.; Ziolek, M. New phospho-silicate and niobo-phospho-silicate MCF materials modified with MPTMS – Structure, surface and catalytic properties. *Micropor. Mesopor. Mat.* **2013**, *181*, 88-98.

(19) Choi, Y. Park, D. S.; Yun, H. J.; Baek, J.; Yun, D.; Yi, J. Mesoporous siliconiobium phosphate as a pure Brønsted acid catalyst with excellent performance for the dehydration of glycerol to acrolein. *ChemSusChem* **2012**, *5*, 2460-2468.

(20) Xi, J.; Xia, Q.; Shao, Y.; Ding, D.; Yang, P.; Liu, X.; Lu, G.; Wang, Y. Production of hexane from sorbitol in aqueous medium over $Pt/NbOPO_4$ catalyst. *Appl. Catal. B Environ.* **2016**, *181*, 699-706.

(21) Sreekumar, S., Balakrishnan, M., Goulas, K.; Gunbas, G.; Gokhale, A. A.; Louie, L.; Grippo A.; Scown, C. D.; Bell, A. T.; Toste, F. D. Upgrading lignocellulosic products to drop-in biofuels via dehydrogenative cross-coupling and hydrodeoxygenation sequence. *ChemSusChem* **2015**, *8*, 2609-2614.

(22) Xia, Q. Chen, Z.; Shao, Y.; Gong, X.; Wang, H.; Liu, X.; Parker, S. F.; Han X.; Yang, S.; Wang, Y. Direct hydrodeoxygenation of raw woody biomass into liquid alkanes. *Nat. Commun.* **2016**, *7*, 11162.

(23) Clayden, N. J.; Accardo, G.; Mazzei, P.; Piccolo, A.; Pernice, P.; Vergara, A.; Ferone C.; Aronne, A. Phosphorus stably bonded to a silica gel matrix through niobium bridges. *J. Mater. Chem. A* **2015**, *3*, 15986-15995.

(24) Carniti, P.; Gervasini, A.; Biella, S.; Auroux, A. Intrinsic and effective acidity study of niobic acid and niobium phosphate by a multitechnique approach. *Chem. Mater.* **2005**, *17,* 6128-6136.

(25) Carniti, P.; Gervasini, A.; Marzo M. Silica–niobia oxides as viable acid catalysts in water: effective vs. intrinsic acidity. *Catal. Today* **2010**, *152*, 42-47.

(26) Carniti, P.; Gervasini, A. Liquid-solid adsorption properties: Measurement of the effective surface acidity of solid catalysts. *Calorimetry and Thermal Methods in Catalysis*. A. Auroux (Ed.), **2013,** *17*, Springer Series in Materials Science, 154.

(27) Tauc, J.; Grigorovici, R.; Vancu, A. Optical properties and electronic structure of amorphous germanium. *Phys. Status Solidi B* **1966**, *15*, 627-637.

(28) He, J., Li; Q.-J.; Fan, Y.-N. Dispersion states and acid properties of SiO_2-supported Nb_2O_5. *J. Solid State Chem.* **2013**, *202*, 121-127.

(29) Zhu, H.; Zheng, Z.; Gao, X.; Huang, Y.; Yan, Z.; Zou, J.; Yin, H.; Zou, Q.; Kable, S. H.; Zhao, J.; et al. Structural evolution in a hydrothermal reaction between Nb_2O_5 and NaOH solution: from Nb_2O_5 grains to microporous $Na_2Nb_2O_6 \cdot {}^2/_3H_2O$ fibers and $NaNbO_3$ cubes. *J. Am. Chem. Soc.* **2006**, *128*, 2373-2384.

(30) Nishimura, M.; Asakura, K.; Iwasawa, Y. New SiO_2-supported niobium monomer catalyst for dehydrogenation of ethanol. *J. Chem. Soc., Chem. Commun.* **1986**, 1660-1661.

(31) Tranca, D. C.; Wojtaszek-Gurdak, A; Ziolek, M.; Tielens, F. Supported and inserted monomeric niobium oxide species on/in silica: a molecular picture. *Phys. Chem. Chem. Phys.* **2015**, *17*, 22402-22411.

(32) Engelhardt, G.; Jancke, H.; Hoebbel, D.; Wieker, W. Strukturuntersuchungen an Silikatanionen in wäßriger Lösung mit Hilfe der ^{29}Si□NMR□Spektroskopie. *Z. Chem.*, **1974**, *14*, 109-110.

(33) Clayden, N. J.; Esposito, S.; Pernice, P.; Aronne, A. Solid State ^{29}Si and ^{31}P NMR study of gel derived phosphosilicate glasses. *J. Mater. Chem.* **2001**, *11*, 936-43.

(34) Hartmeyer, G.; Marichal, C.; Lebeau, B.; Rigolet, S.; Caullet, P.; Hernandez, J. Speciation of silanol groups in precipitated silica nanoparticles by ^{1}H MAS NMR spectroscopy. *J. Phys. Chem. C* **2007**, *111*, 9066-9071.

(35) Fleischer, U.; Kutzelnigg, W.; Bleiber, A.; Sauer, J. Proton NMR chemical shift and intrinsic acidity of hydroxyl groups. Ab initio calculations on catalytically active sites and gas-phase molecules. *J. Amer. Chem. Soc.* **1993**, *115*, 7833-7838.

(36) Xue, X.; Kanzaki, M. Ab initio calculation of the ^{17}O and ^{1}H NMR parameters for various OH groups: implications to the speciation and dynamics of dissolved water in silicate glasses. *J. Phys. Chem. B* **2001**, *105*, 3422-3434.

(37) Papulovskiy, E.; Khabibulin, D. F.; Terskikh, V. V.; Paukshtis, E. A.; Bondareva, V. M.; Shubin, A. A.; Andreev, A. S.; Lapina, O. Effect of impregnation on the structure of niobium oxide/alumina catalysts studied by multinuclear Solid-State NMR, FTIR, and quantum chemical calculations. *J. Phys. Chem. C* **2015**, *119*, 10400 -10411.

(38) Moreau, C.; Durand, R.; Roux, A.; Tichit, D. Isomerization of glucose into fructose in the presence of cation-exchanged zeolites and hydrotalcites. *Appl. Catal. A: Gen.* **2000**, *193*, 257-264.

(39) Moreau, C.; Belgacem, M. N.; Gandini, A. Recent catalytic advances in the chemistry of substituted furans from carbohydrates and in the ensuing polymers. *Top. Catal.* **2004**, *27*, 1-30.

(40) Román-Leshkov, Y.; Moliner, M.; Labinger, J. A.; Davis, M. E. Mechanism of glucose isomerization using a solid Lewis acid catalyst in water. *Angew. Chem., Int. Ed.* **2010**, *49*, 8954-8957.

(41) Abdulbari, H. A.; Akindoyo, E. O.; Mahmood, W. K. Renewable resource-based lubricating greases from natural and synthetic sources: insights and future challenges. *Chem. Bio. Eng. Rev.* **2015**, *2*, 406-422.

(42) Di Serio, M.; Tesser, R.; Pengmei, L.; Santacesaria, E. Heterogeneous catalysts for biodiesel production. *Energ. Fuels* **2003**, *22*, 207-217.

(43) Borges, M. E.; Díaz, L. Recent developments on heterogeneous catalysts for biodiesel production by oil esterification and transesterification reactions: a review. *Renew. Sust. Energ. Rev.* **2012**, *16*, 2839-2849.

(44) Kuzminsk, M.; Backov, R.; Gaigneaux, E. M. Behavior of cation-exchange resins employed as heterogeneouscatalysts for esterification of oleic acid with trimethylolpropane. *Appl. Catal. A: Gen.* **2015**, *504*, 11-16.

(45) Oh, J.; Yang, S.; Kim, C.; Choi, I.; Kim, J. H.; Lee, H. Synthesis of biolubricants using sulfated zirconia catalysts. *Appl. Catal. A: Gen.* **2013**, *455*, 164-171.

(46) Wu, Y.; Li, W.; Wang, X. Synthesis and properties of trimethylolpropane trioleate as lubricating base oil. *Lubrification Science* **2015**, *27*, 369-379.

(47) Santacesaria, E.; Ambrosio, M.; Sorrentino, A.; Tesser, R.; Di Serio M. Double bond oxidative cleavage of monoenic fatty chains. *Catal. Today* **2003**, *79*, 59-65.

TABLES

Table 1. UV-vis-DRS curve fitting. Wavelength, λ (nm), estimated relative intensities, I, full width at half maximum, F_w (nm), calculated from line fitting of the UV-vis-DRS spectra. Standard errors are ± 1 nm in λ, ±2 in the intensity, and ±3 nm in the linewidth.

Sample	λ (nm)	I	F_w (nm)
2.5NbP-500	196	30	65
	231	21	43
	266	31	45
	300	18	39
2.5NbP-500w	199	23	44
	230	27	42
	264	31	41
	295	19	38

Table 2. ^{31}P curve fitting. Chemical shifts, δ (ppm), estimated relative intensities, I, and full width at half maximum, F_w (ppm), calculated from line fitting of the ^{31}P resonances. Standard errors are ± 0.25 ppm in δ, ±1.0 in the intensity, and ±0.25 ppm in the linewidth.

Sample	δ (ppm)	I	F_w (ppm)
2.5NbP-500	-0.04	1.0	2.6
	-8.9	46.0	8.8
	-21.1	43.0	8.5
	-35.1	10.0	7.8
2.5NbP-500w	-0.4	2.5	5.3
	-9.6	19.8	7.4
	-20.6	65.5	9.8
	-36.4	12.2	7.6

Table 3. Determination of the nature of the acid sites determined by FT-IR with pyridine (Py) as probe molecule in absence and in presence of water. [a]

Sample	$Py_{(vap)}$ [b]			$Py_{(aq)}$ [c]		
	LAS (meq g^{-1})	BAS (meq g^{-1})	LAS/BAS	LAS (meq g^{-1})	BAS (meq g^{-1})	LAS/BAS
NbP	0.082	0.039	2.10	0.061	0.036	1.69
2.5 NbP-500	0.088	0.083	1.06	0.027	0.069	0.39

[a] All the values have been determined after thermal desorption of pyridine at 100 °C.

[b] Pyridine contacted in vapor phase. [c] Pyridine contacted in aqueous solution.

Table 4. Kinetic coefficients evaluated at three representative temperatures and Arrhenius parameters for the catalytic hydrolysis of inulin.

Sample	k_T (mequiv·g^{-1}·min^{-1})			E_a (kJ·mol^{-1})	Ln A[a]
	T=60 °C	T=70 °C	T=80 °C		
NbP					
fresh	0.0124	0.0567	0.2370	144.1 ± 11.5	48.6 ± 3.9
water stabilized	0.00614	0.0278	0.1155	143.5 ± 4.4	46.7 ± 1.5
2.5NbP-500					
fresh	0.0160	0.0712	0.2907	141.7 ± 8.2	47.0 ± 2.8
water stabilized					

[a] A expressed in mequiv·g^{-1}·min^{-1}

FIGURES

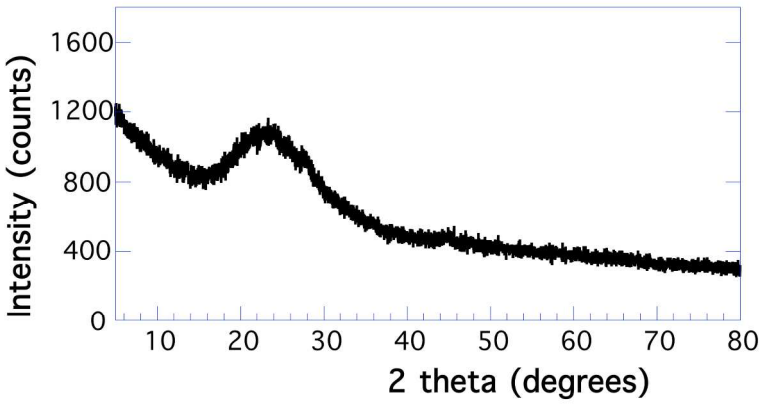

Figure 1. PXRD pattern of the 2.5NbP-500 sample.

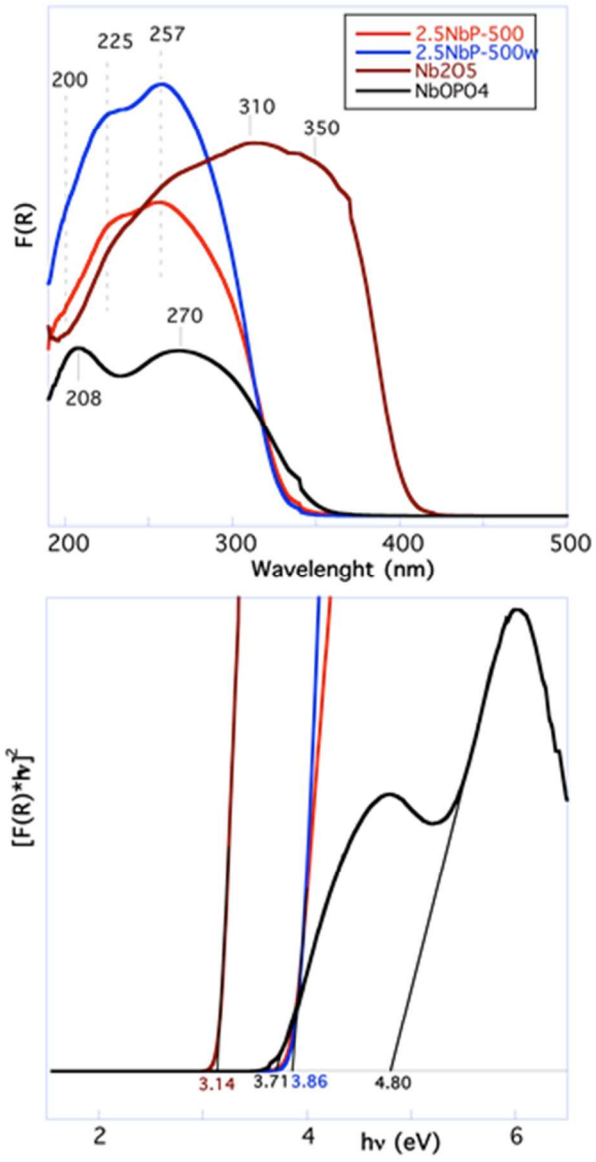

Figure 2. UV-Vis-DRS (top) and the corresponding Tauc plot (bottom) of the investigated samples. The same Eg was observed for 2.5NbP-500 and 2.5NbP-500w (Eg = 3.86 eV), demonstrating that the water treatment does not modify the distribution of surface Nb species

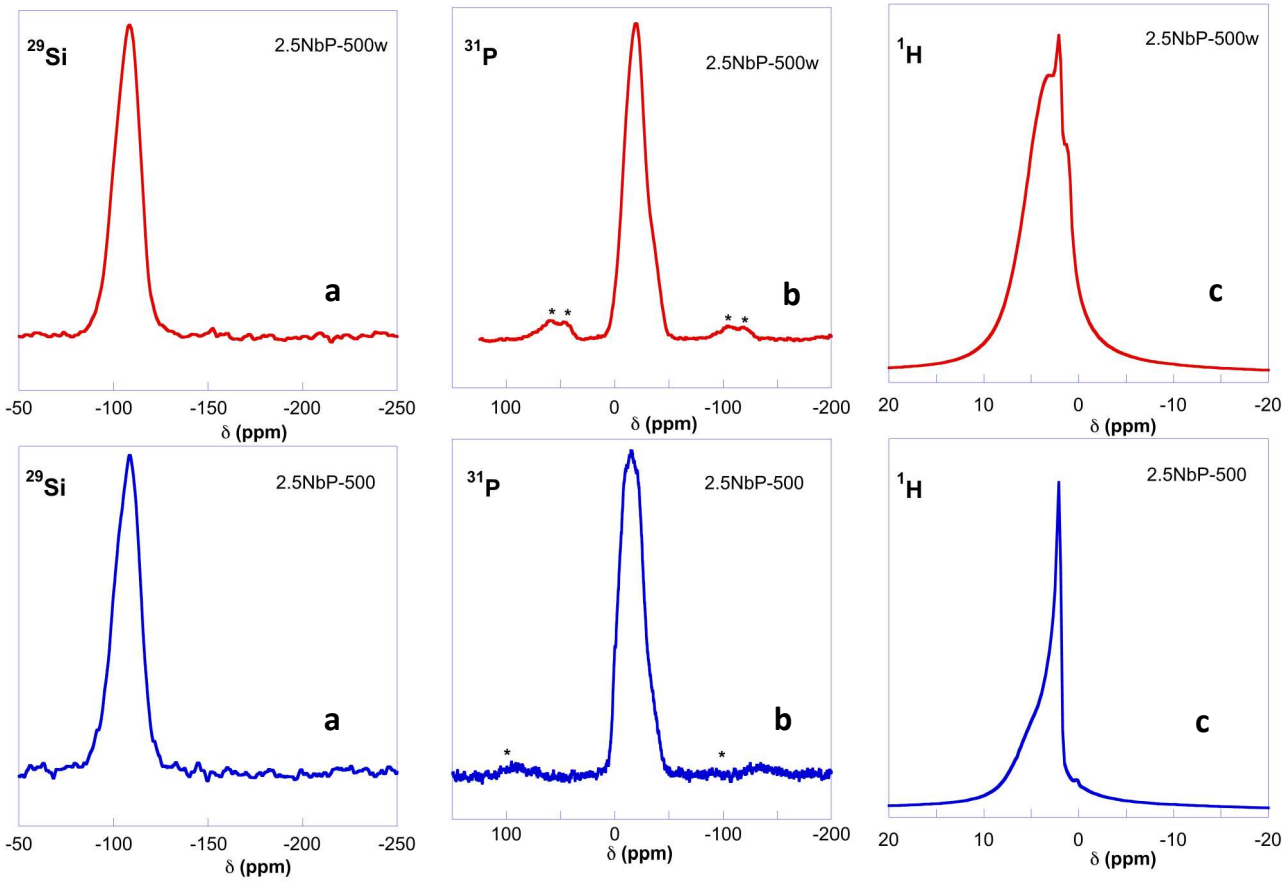

Figure 3. MAS NMR ^{29}Si (a), ^{31}P (b) and ^{1}H (c) of the investigated 2.5NbP-500w (top) and 2-5NbP-500 (bottom) samples. High stability in water is suggested by ^{29}Si spectra, changes are seen only in ^{31}P and ^{1}H spectra indicating the hydrolysis of few high reactive sites.

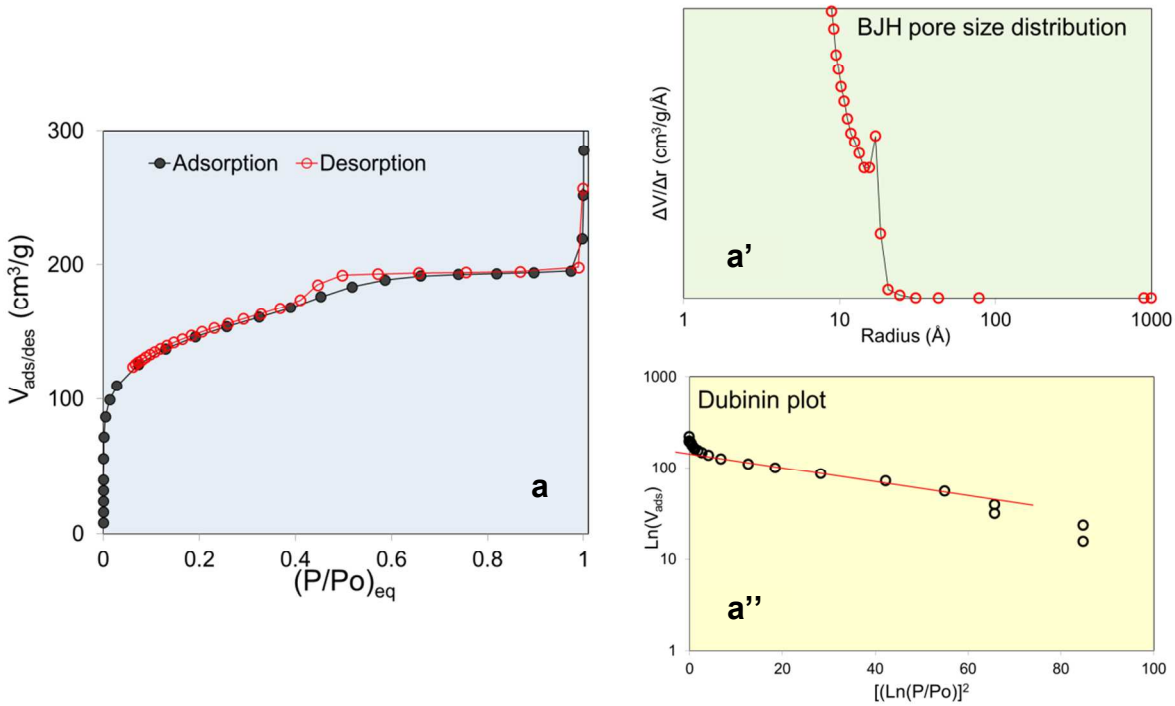

Figure 4. Morphologic characterization of 2.5NbP-500 sample. N_2 adsorption and desorption isotherms at -196 °C (a), pore size distribution determined by BJH model equation from the desorption branch of the N_2-isotherms (a'), and Dubinin plot for the determination of the micropore volume (a'').

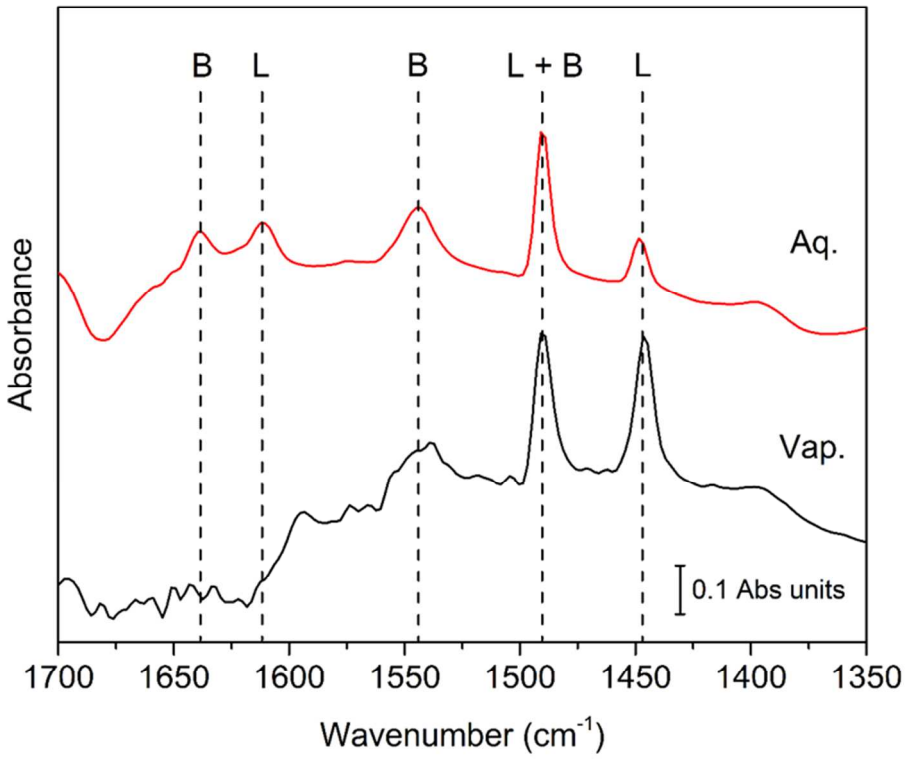

Figure 5. FT-IR desorption spectra of pyridine on 2.5NbP-500 sample at 100 °C with pyridine adsorbed in vapor phase (Vap.) and in aqueous solution (Aq.). Quantitative determinations of Brønsted (BAS) and Lewis (LAS) acid sites were made on the peaks at 1540 and 1448 cm^{-1}, respectively.

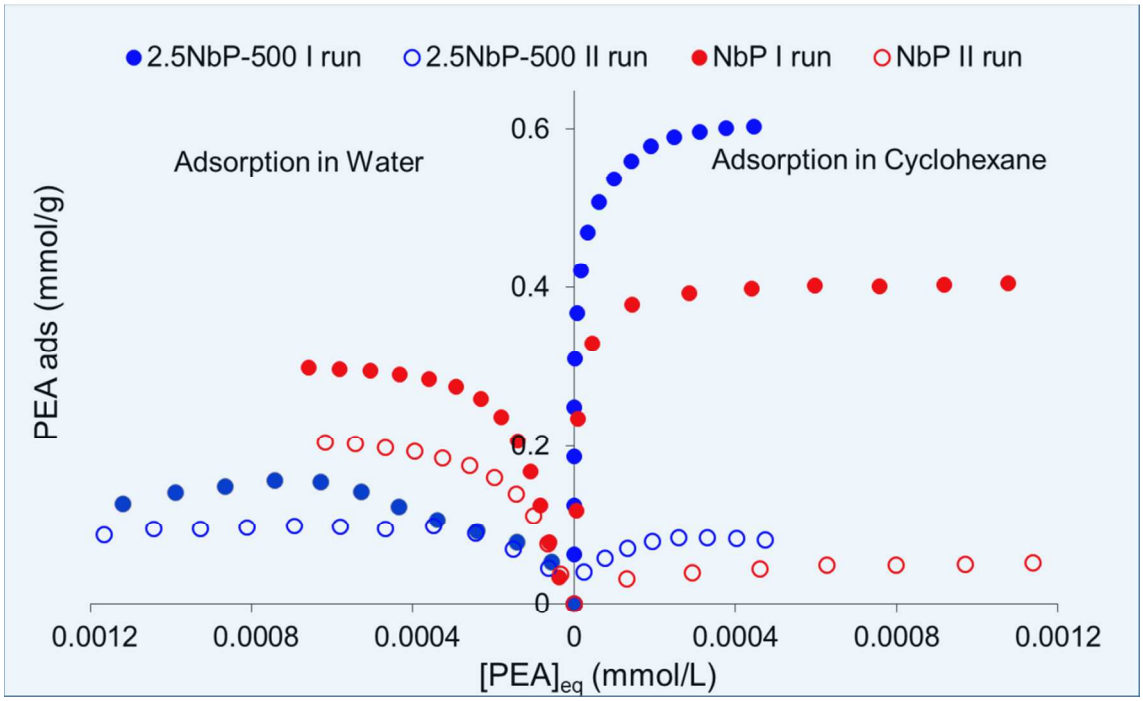

Figure 6. Surface acid characterization of the studied samples. Adsorption isotherms of phenylethylamine (PEA) at 30 °C on 2.5NbP-500 and NbP (reference sample), measured in two different liquids: cyclohexane for the *intrinsic* acidity determination and water for the *effective* acidity determination; first run (on the fresh sample) and second run (on the sample with PEA chemically adsorbed) are shown.

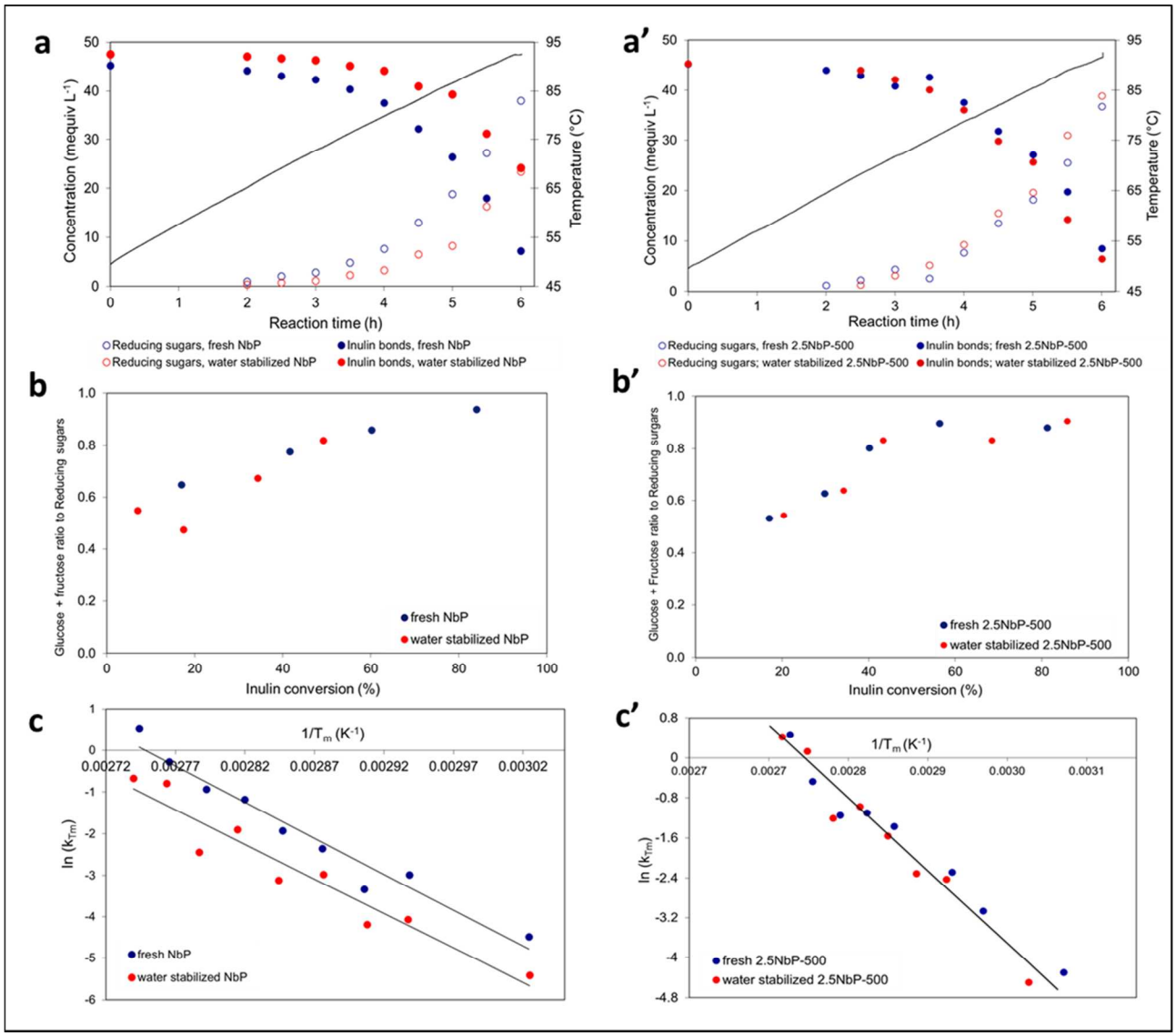

Figure 7. Catalytic performances of NbP and 2.5NbP-500 in the inulin hydrolysis. Concentration of total reducing sugars formed and of residual inulin bonds as a function of time and temperature (second axis) on fresh and water stabilized NbP (a) and 2.5NbP-500 (a'). Selectivity to monosaccharides: ratio between glucose plus fructose and total reducing sugars as a function of inulin conversion on fresh and water stabilized NbP (b) and 2.5NbP-500 (b'). Arrhenius plot for the reaction of inulin hydrolysis determined in the temperature range 50-90 °C on fresh and water stabilized NbP (c) and 2.5NbP-500 (c'); T_m represents the average temperature during ca. 30 min of reaction corresponding to ca. ΔT=5 °C.

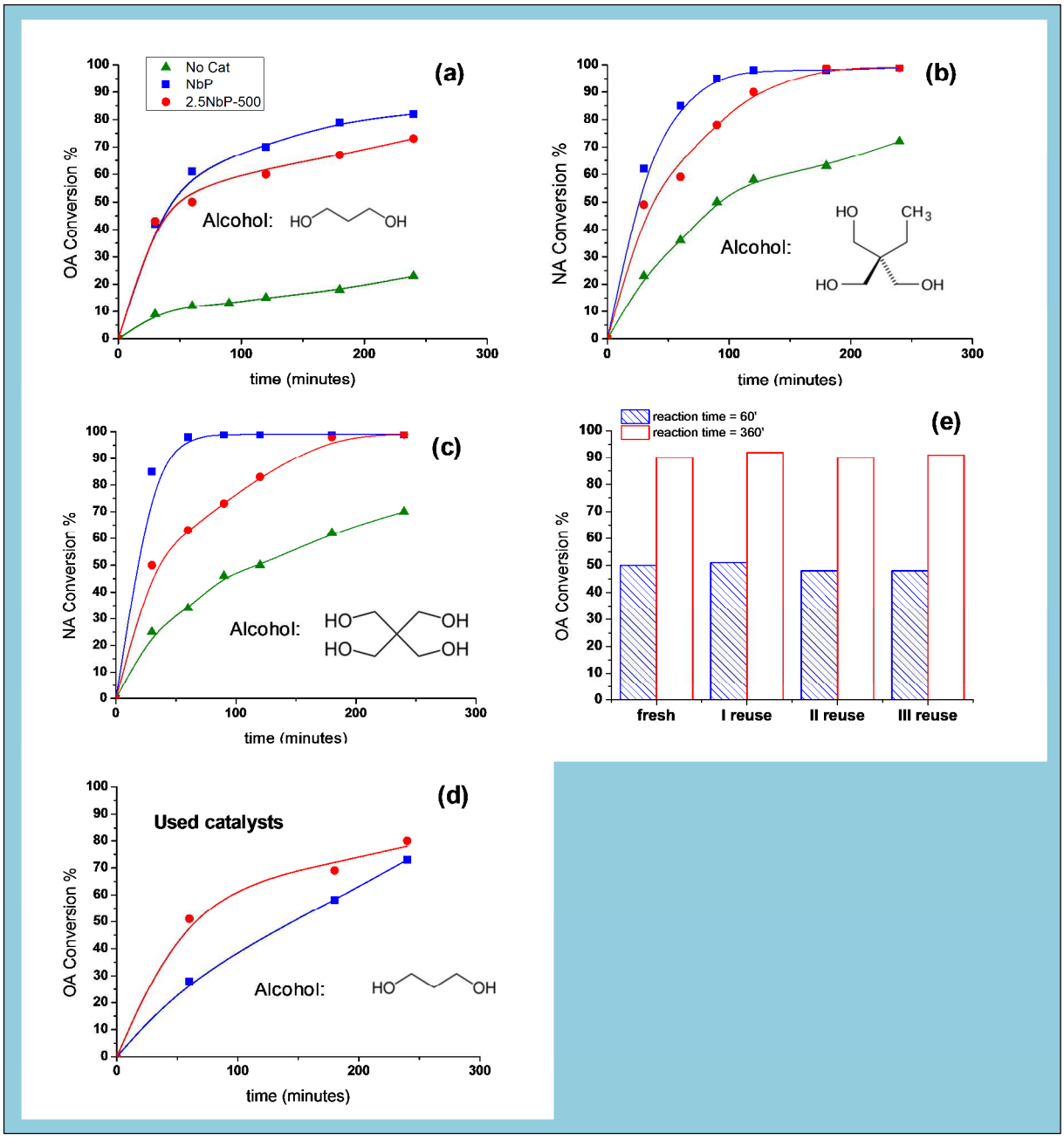

Figure 8. Catalytic performances of NbP and 2.5NbP-500 in the esterification reaction. Esterification runs, conversion of fatty acids. Reaction conditions: T= 180°C, catalyst = 1% wt on reaction mixture, molar ratio fatty acid/alcohol = 2/1 (a), (d) and (e); 3/1 (b); 4/1 (c). Oleic Acid (OA), 1,3 propanediol, (a) and (d); nonanoic acid, trymethylolpropane (b); nonanoic acid, pentaerythritol (c). Results obtained in the I reuse of catalysts (d). Results obtained with fresh 2.5NbP-500 catalyst and in the successive 3 runs (Oleic Acid, 1,3 propanediol) (e).

TOC Graphic

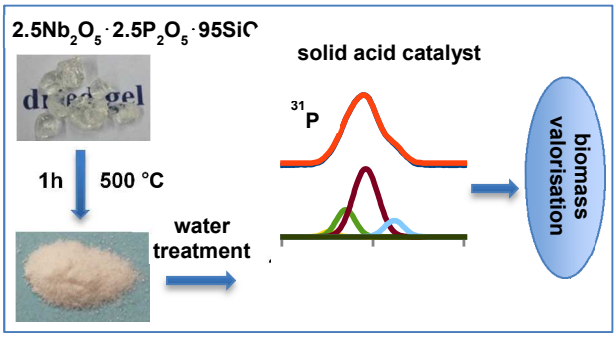
2.5Nb2O5·2.5P2O5·95SiO
solid acid catalyst
dried gel
31P
1h
500 °C
water
treatment
biomass
valorisation